Econ. Environ. Geol.
Vol. 32, No. 6 p. 561-573, 1999.

Fluid Inclusion and Stable Isotope Studies of Mesothermal Gold Vein Deposits in Metamorphic Rocks of Central Sobaegsan Massif, Korea : Youngdong Area

Chil-Sup So*, Seong-Taek Yun* and Soon-Hak Kwon*

ABSTRACT : Mesothermal gold deposits of the Heungdeok, Daewon and Ilsaeng mines in the Youngdong area occur in fault shear zones in Precambrian metamorphic rocks of central Sobaegsan Massif, Korea, and formed in single stage of massive quartz veins (0.3 to 3 m thick). Ore mineralogy is simple, consisting dominantly of pyrrhotite, sphalerite and galena with subordinate pyrite, chalcopyrite, electrum, tetrahedrite and native bismuth. Fluid inclusion data indicate that hydrothermal mineralization occurred at high temperatures (>240° to 400°C) from H_2O-CO_2(-CH_4)-NaCl fluids with salinities less than 12 wt. % equiv. NaCl. Fluid inclusions in vein quartz comprise two main types. These are, in decreasing order of abundance, type I (aqueous liquid-rich) and type II (carbonic). Volumetric proportion of the carbonic phase in type II inclusions varies widely in a single quartz grain. Estimated CH_4 contents in the carbonic phase of type II inclusions are 2 to 20 mole %. Relationship between homogenization temperature and salinity of fluid inclusions suggests a complex history of fluid evolution, comprising the early fluid's unmixing accompanying CO_2 effervescence and later cooling. Estimated pressures of vein filling are at least 2 kbars. The ore mineralization formed from a magmatic fluid with the $\delta^{34}S_{\Sigma S}$, $\delta^{18}O_{water}$ and δD_{water} values of -2.1 to 2.2‰, 4.7 to 9.3‰ and -63 to -79‰, respectively. This study validates the application of a magmatic model for the genesis of mesothermal gold deposits in Youngdong area.

INTRODUCTION

Mesothermal gold deposits worldwide recently have been the major target of active exploration and genetic study. However, the fluid source and genetic environments of mesothermal gold deposits are remained elusive and controversial. In many of the mesothermal gold deposits the metamorphic source model has been widely proposed for the fluids. Recently however, the magmatic model (e.g., Burrows *et al.*, 1986; Spooner, 1991) and the meteoric water model (e.g., Nesbitt, Muehlenbachs, 1989) also have been proposed. Along the eastern edge of the Sino-Korean platform, the occurrence of many mesothermal gold deposits is recently known and pulls the great scientific and economic interest. These deposits in eastern China are considered to have formed from magmatic fluids during Mesozoic tectono-magmatic reactivation of the edge of the Archean North China Craton (e.g., Trumbull *et al.*, 1992; Miller *et al.*, 1998; Zhang *et al.*, 1999).

The occurrence of mesothermal-type gold deposits also has been recently documented in Precambrian metamorphic rocks of central part of southern Korea, including the Jungwon (Shelton *et al.*, 1988) and Youngdong areas (Yun, 1991; So *et al.*, 1995; So, Yun, 1997). These deposits share common features which include (1) the host rock petrography, largely Precambrian paragneiss, (2) the Jurassic age of mineralization, ranging from 146 to 166 Ma, (3) the association with weak hydrothermal alteration, and (4) the volumetrically low sulfide concentration and simple sulfide mineralogy, including pyrrhotite± pyrite, base-metal sulfides and gold-rich electrums. Fluid inclusion and stable isotope studies have suggested that these mesothermal deposits formed from CO_2-rich fluids with high temperatures, 290° to 375°C for Jungwon area and 220° to 480°C for Youngdong area. According to Yao *et al.* (1999), these data for Korean deposits are comparable with those of mesothermal gold deposits in eastern edge of the Sino-Korean platform.

The Youngdong area, located approximately 180 km southeast of Seoul, forms one of the important

* Dept. of Earth & Env. Sci., Korea Univ., Seoul 136-701, Korea, E-mail: styun@kucc.08.korea.ac.kr

gold-silver mineralized district in South Korea, in which different genetic types of gold-silver deposits occur. These are metamorphic rock-hosted gold deposits, granite-hosted gold-silver deposits, and volcanic rock-hosted silver-gold deposits. The metamorphic rock-hosted gold deposits, including those of the Samhwanghak and Samdong mines, are considered to have formed from mesothermal-type fluids genetically related to the Jurassic Daebo orogeny (Yun, 1991; So *et al.*, 1995; So, Yun, 1997). In order to convince the origin and genetic environments of metamorphic rock-hosted mesothermal gold deposits in central Korea, fluid inclusions and stable isotopes of gold deposits in the Heungdeok, Daewon and Ilsaeng mines are studied in this paper. These mines have not been studied. The results of this study will be helpful to understand the genesis of mesothermal gold deposits in south Korea and in edge parts of the Sino-Korean Platform in tectonic viewpoint.

ORE DEPOSITS

At least sixteen quartz veins of the Heungdeok, Daewon and Ilsaeng mines are hosted in Precambrian metamorphic rocks of the Sobaegsan massif (see Fig. 1 for the setting of principal veins). These mines have been exploited actively during 1910s to 1960s but is now abandoned. Annual gold production during 1940s was 1.4 to 43 kg from each mine, with average ore grades of about 6 to 13 g/ton Au. Remained ore reserves are totally estimated to be about 180,000 metric tons (Kim *et al.*, 1982). The metamorphic rocks in the mine area comprise banded biotite gneiss and granitic gneiss. These two rocks commonly show gradual contacts. Banded biotite gneiss is locally migmatitic. These metamorphic rocks yielded a whole-rock Rb-Sr age of 1,810±10 Ma (Choo, Kim, 1985), and show the metamorphic mineral assemblages of amphibolite facies.

Gold-bearing quartz veins fill the NE- or NW-trending fault shear zones with steep dips (60~70°), and can be traced up to >0.5 km. The veins of the each mine are subparallel each other and commonly to the foliation of host rocks, and show similar morphology and mineralogy. Vein thickness is varied considerably from <0.3 to 3 m. Narrow (usually <0.5 m thick), weak hydrothermal alteration zones with an assemblage of chlorite, sericite, siderite and albite is recognized in wall rock adjacent to veins. Earthy graphite often occurs along mineralized fault planes.

Mineralogy and paragenesis of veins are quite similar among the Heungdeok, Daewon and Ilsaeng deposits and are shown in Fig. 2. Ore mineralization occurs in single stage quartz veins which are massive in occurrence. The ore mineralogy is very simple, consisting mainly of iron- and base-metal sulfides. Sulfide minerals are rare in amounts (usually <10 vol. % of vein) and largely occur within small healed fractures cutting quartz matrix.

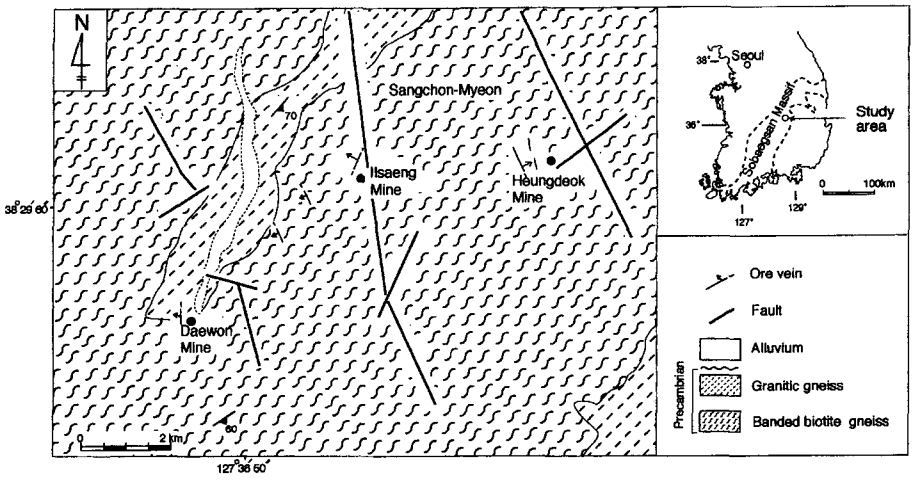

Fig. 1. General geologic map of the study area in the central Sobaegsan Massif of Korea.

This relationship indicates that deposition of sulfide minerals largely occurred after deposition of quartz. Ore minerals consist mainly of pyrrhotite, sphalerite (X_{FeS} = 0.10~0.17), chalcopyrite and galena with rare amounts of electrum, native bismuth and tetrahedrite. Pyrrhotite and dark brown to black sphalerite are characteristic of veins and are closely intergrown each other. Gold grains (usually <0.1 mm long) are associated with sufide-rich fractures, and occur as anhedral gold-rich electrums (74 to 83 atom. % Au) in association with galena, chalcopyrite, tetrahedrite and native bismuth. Gold content of electrum grains is very uniform without any compositional zoning.

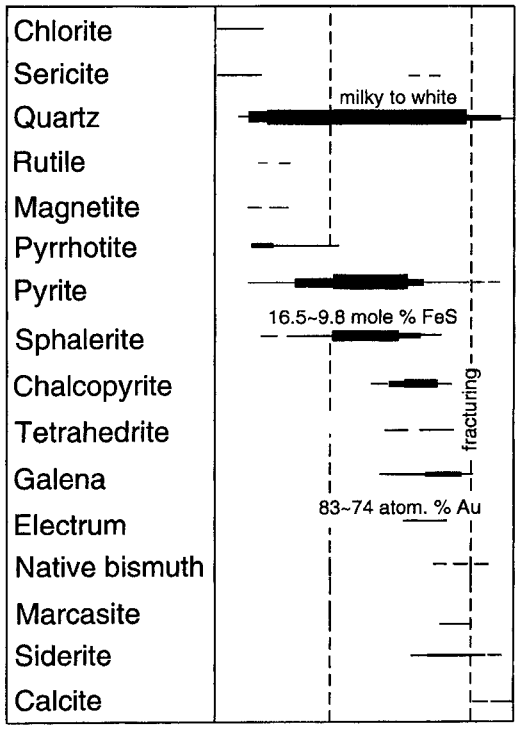

Fig. 2. Generalized paragenetic sequence of alteration and vein minerals from the Heungdeok, Daewon and Ilsaeng gold mines.

FLUID INCLUSIONS

About 60 vein samples were collected from underground and surface area, and about 600 fluid inclusions were examined for fluid inclusion study. Vein quartz was usually inclusion-rich, whereas sphalerite was not suitable for fluid inclusion study due to its opacity. Microthermometric data were obtained on a FLUID Inc. gas-flow heating/freezing stage which was calibrated with synthetic CO_2 and H_2O inclusions and various organic solvents. Salinity data reported are based on freezing-point depression in the system H_2O-NaCl for H_2O-rich inclusions (Bodnar, 1993) and on clathrate melting temperatures for clathrate-forming and liquid CO_2-bearing (carbonic) inclusions (Bozzo *et al.*, 1975; Diamond, 1992). Temperatures of total homogenization have standard errors of ±1.0°C. Both the melting tem-

Table 1. Summary of microthermometric data of fluid inclusions in vein quartz from Au deposits in the Youngdong area of the central Sobaegsan Massif.

Mine	Inclusion type	Occurrence[1]	Tm-CO_2 (°C)	Th-CO_2 (°C)	Tm-clathrate (°C)	Tm-ice (°C)	Th-total (°C)	Estimated salinity (wt. % NaCl)
Heungdeok	Ia	P-	-	-	-	-1.,8~-5.6	244~401	3.1~8.7
	Ib	S	-	-	-	-0.2~-7.7	153~244	0.4~11.3
	IIa	P	-62.9~-56.6	19.8~29.7	6.5~11.0	-	264~343	0.2~5.8
	IIb	P	-62.8~-58.8	9.8~25.8	6.4~9.1	-	266~304	1.8~6.8
Daewon	Ia	P	-	-	-	-0.9~-5.8	245~358	1.2~9.0
	Ib	P	-	-	-	-1.8~-6.2	151~241	1.0~10.2
	IIa	P	-62.6~-57.2	8.4~26.7	5.8~9.2	-4.2	275~357	1.6~7.8
	IIb	P	-63.3~-58.3	14.3~27.7	6.3~9.2	-	256~358	1.6~7.0
Ilsaeng	Ia	P	-	-	-	-1.0~-4.8	249~401	1.3~7.6
	Ib	S	-	-	-	-0.6~-7.2	152~238	1.1~10.7
	IIa	P	-6.2~-56.6	8.9~21.0	4.7~11.6	-	152~238	0.0~7.8
	IIb	P	-59.8~-58.9	20.8~27.6		-	310~322	3.0~5.4

[1] Based on normal criteria of Roedder (1984). P = primary; S = obvious secondary.
Ia = aqueous, liquid-rich (primary); Ib = aqueous, liquid-rich (secondary); IIa = CO_2(-CH_4)-bearing(CO_2<H_2O); IIb = CO_2(-CH_4)-bearing(CO_2>H_2O)

peratures of frozen carbonic phase, ice and clathrate and the homogenization temperatures of carbonic phase have standard errors of ±0.2°C. In addition to the measurements of microthermometric data (Table 1), the mole fraction of each fluid phase was determined visually for some inclusions.

Types of fluid inclusions

Vein quartz samples are inclusion-rich, probably due to the repeated fracturing and healing during and after the quartz deposition. The size of fluid inclusions ranges from <3 to 25 μm. Two major types of fluid inclusions are identified on the basis of phase relations and cooling behavior. These are type I (aqueous liquid-rich) and type II (carbonic) inclusions, as shown in Fig. 3.

Type I inclusions occupies about 70% of the numbers of fluid inclusions, and comprise H_2O-rich, liquid and vapor at room temperature. The gas bubble occupies <10 to 45% of the total inclusion volume. Some type I inclusions recognizably formed CO_2 clathrates during freezing runs, and are classified into type Ia inclusions. Type Ib inclusions seem to purely water-rich without the formation of clathrate, and occur as clusters along healed fractures (Fig. 3D). Based on the criteria of Roedder (1984), type I inclusions are both primary and secondary in origin.

Type II inclusions consist of three (water+carbonic liquid+carbonic vapor) or two (water+carbonic liquid) phases at room temperature. With slight cooling down to 0°C, however, a carbonic vapor also forms in two phase type II inclusions. Type II inclusions can be classified into two subtypes, according to the relative volumetric abundance of carbonic phase at 0~20°C: type IIa (H_2O>CO_2) and type IIb (CO_2>H_2O). The volumetric proportion

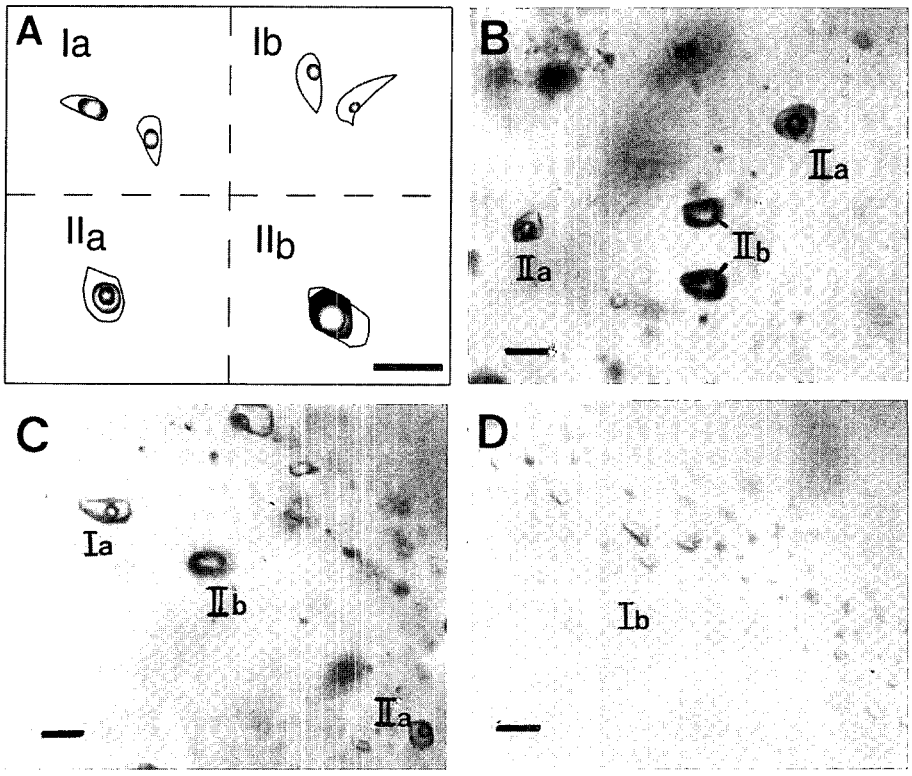

Fig. 3. Occurrence and compositional type of fluid inclusions in vein quartz. A. Sketches of types of fluid inclusions. Type I = aqueous liquid-rich inclusions (Ia = CO_2 clathrate-forming; Ib = purely aqueous); Type II = carbonic inclusions (IIa = H_2O>CO_2 in volume; IIb = H_2O<CO_2). B. Photomicrograph showing the coexistence of type IIa and type IIb inclusions (Heungdeok mine). C. The coexistence of type IIa, type IIb, type Ia inclusions (Daewon mine). D. The cluster of fracture-controlled (secondary) type Ib inclusions (Ilsaeng mine). Scale bars are 10 μm long.

of carbonic phase (liquid+vapor) at 25°C are about 10 to 35% (mostly between 15 and 20%) for type IIa inclusions and about 65 to 90% for type IIb inclusions. The whole range of carbonic phase volume is usually observed within a quartz grain. Type IIb inclusions comprise about 10% of type II inclusions. Except for rare type IIb inclusions occurring along healed fractures, type II inclusions are mostly regular in shape with no planar orientation (Fig. 3B, C). This occurrence indicates the primary origin for most type II inclusions (Roedder, 1984).

All of type Ia and type IIa inclusions and most type IIb inclusions appear to be primary, whereas type Ib inclusions are predominantly secondary (Fig. 3B, C, D). However, it is impossible to establish consistently the fluid inclusion chronology due to repeated fracturing and healing. Therefore, in this study we have employed a more practical distinction between primary+pseudosecondary (P+PS) and obvious secondary (S).

Heating and freezing data

Type I inclusions

The first ice melting of type I inclusions occurred at temperatures near -21°C (although it was so difficult to be observed), possibly indicating the dominance of NaCl among dissolved salts (Borisenko, 1977; Crawford, 1981). Temperatures of final ice melting (Tm-ice) in type Ia inclusions range from -0.9° to -5.8°C, corresponding to salinities of 1.2 to 9.0 wt. % NaCl equiv (Fig. 4). The Th-total data of P+PS type I inclusions range from 244° to 401°C (Fig. 5). Secondary type Ib inclusions did not nucleate recognizable clathrates upon cooling, suggesting the poverty of CO_2 (<2.7 wt. % CO_2 if present; Hedenquist, Henley, 1985). The Tm-ice values of type Ib inclusions range from -0.2° to -7.7°C, corresponding to salinities of 0.2 to 11.3 wt. % NaCl equiv (Fig. 4). They have the Th-total values of 153° to 244°C (Fig. 5).

Type IIa inclusions

After the cooling down to about -100°C, melting of the solid CO_2 (Tm-CO_2) occurred at temperatures between -62.9° to -56.6°C (Fig. 6). The low Tm-CO_2 values suggest the presence of CH_4 in addition to CO_2 in carbonic phase (Burruss, 1981; Heyen *et al.*, 1982). Homogenization of the carbonic phase (Th-CO_2) occurred to a liquid at temperatures from 14.3° to 29.7°C (Fig. 6). The Th-CO_2 values were much variable within a single sample, suggesting the variation of the density of carbonic phase at the time of entrapment. Melting temperatures of clathrate (Tm-clathrate) range from 4.7° to 11.6°C (Fig. 6). The Tm-clathrate values of >10.0°C are larger than that of pure CO_2 (Bozzo *et al.*, 1975). This may be due to the presence of CH_4, because the formation of CH_4 clathrate ($CH_4 5H_2O$) would raise the clathrate melting temperature (Hollister, Burruss, 1976; Burruss, 1981). Unfortunately, there is no available data on the relationship between Tm-clathrate value and salinity for H_2O-CO_2-CH_4-NaCl system. Assuming a H_2O-CO_2-NaCl system for type IIa inclusions, these Tm-clathrate values may indicate the low salinity (<9.5 wt. % NaCl equiv.). A small number of total

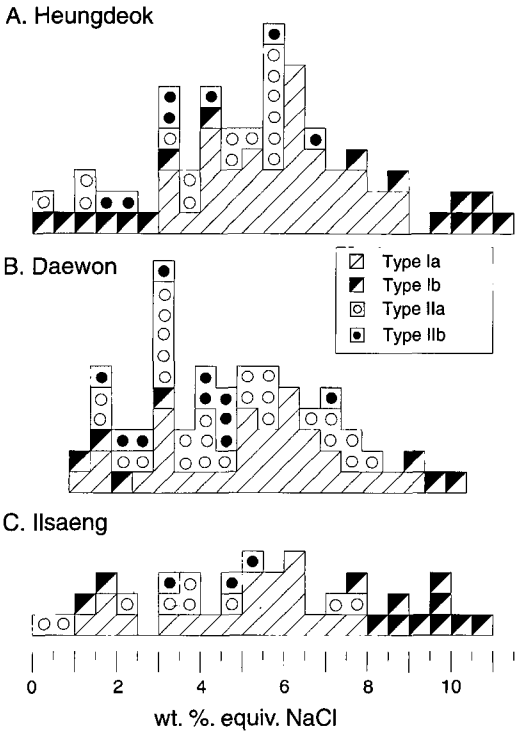

Fig. 4. Frequency diagrams of salinity of fluid inclusions in vein quartz. For the type II inclusions, salinity estimates are reported by assuming a simple H_2O-CO_2-NaCl system without CH_4. Type I = aqueous liquid-rich inclusions (Ia = CO_2 clathrate-forming; Ib = purely aqueous); Type II = carbonic inclusions (IIa = $H_2O > CO_2$ in volume; IIb = $H_2O < CO_2$).

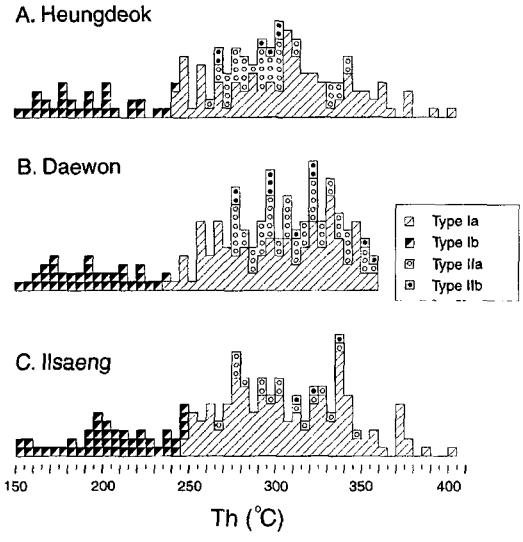

Fig. 5. Frequency diagrams of total homogenization temperature of fluid inclusions in vein quartz. Symbols of fluid inclusion type are the same as in Fig. 4.

homogenization temperatures (Th-total) were obtained because most type IIa inclusions examined decrepitated prior to the total homogenization. The obtained Th-total data range from 264° to 357°C (Fig. 5).

Type IIb inclusions

The Tm-CO_2 values range from -63.3° to -58.3°C (Fig. 6). The Th-CO_2 (to a liquid) values range widely from 8.4° to 26.7°C (Fig. 6). The Th-clathrate values have the range of 6.3° to 9.2°C (Fig. 6). For a H_2O-CO_2-NaCl system, these Th-clathrate values correspond to salinities of 1.6 to 7.0 wt. % NaCl equiv. (Fig. 4). The Th-total values obtained range from 256° to 358°C (Fig. 5).

Bulk composition of type II inclusions

Bulk composition and density of type II inclusions can be estimated from data on the relative volumes of the carbonic and aqueous phases, combined with microthermometric data. The relative volumes of the carbonic and aqueous phases were estimated by measuring the inclusions with a graduated ocular (Roedder, 1984). Assuming that CH_4 is the sole agent responsible for the observed depressions of Tm-CO_2 and Th-CO_2 values (relative to those of pure CO_2), the quantitative V-X_{CH4} projection of

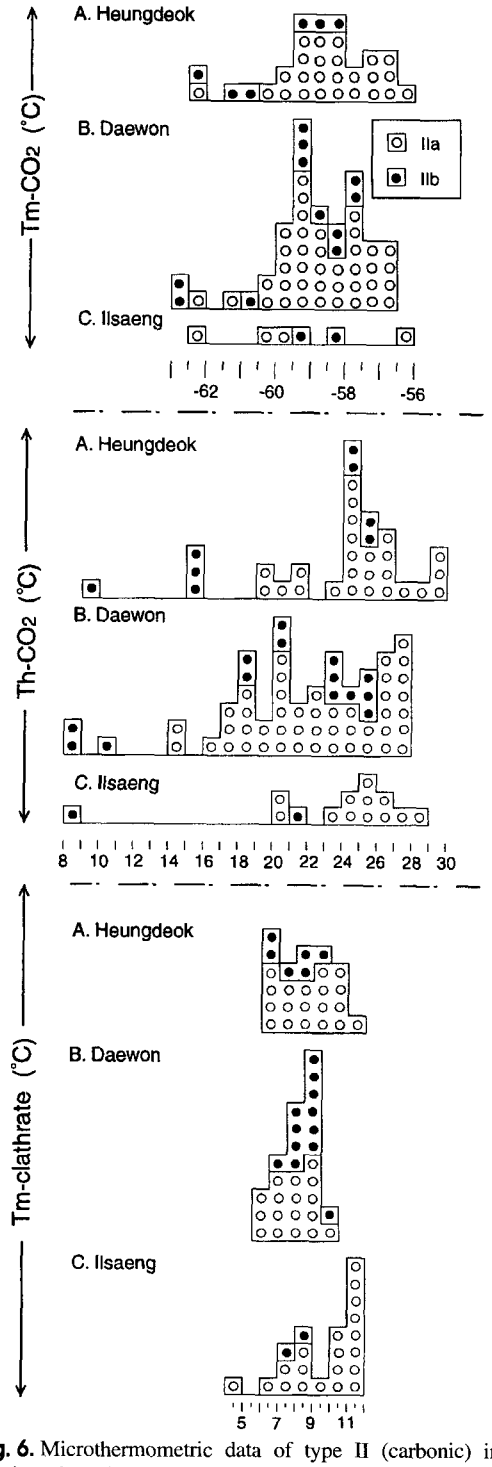

Fig. 6. Microthermometric data of type II (carbonic) inclusions in vein quartz. Tm-CO_2=melting temperature of CO_2; Th-CO_2=homogenization temperature of CO_2; Tm-clathrate=melting temperature of clathrate. Symbols of fluid inclusion type are the same as in Fig. 4.

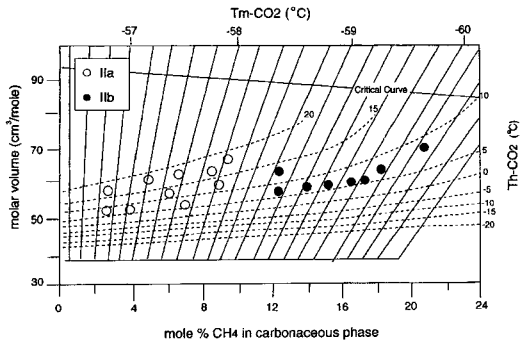

Fig. 7. Molar volume versus mole % CH_4 diagram for the system CO_2-CH_4 system (after Heyen *et al.*, 1982). Semi-quantitative estimates of CH_4 contents in carbonic phase of type II inclusions in vein quartz, based on the melting and homogenization temperatures of carbonic phase, are shown. Symbols of fluid inclusion type are the same as in Fig. 4.

the CO_2-CH_4 system (Heyen *et al.*, 1982), combined with the obtained Tm-CO_2 and Th-CO_2 data, was used to estimate the CH_4 contents in the carbonic phase of type II inclusions. The estimated CH_4 contents range from <4 to 20 mole % (type IIa, 11 to 20 mole %; type IIb, <4 to 18 mole %; Fig. 7).

Densities of the carbonic phase ($\rho_{carb.}$) in type II inclusions can be estimated using the Th-CO_2 data and estimated mole % CH_4 (Angus *et al.*, 1973; Hollister, 1981). Similarly, densities of the aqueous phase can be estimated by extrapolation of the phase diagram for the system H_2O-NaCl (Roedder, Bodnar, 1980). Bulk densities (ρ_{total}) of some type II inclusions were calculated from the densities and volumes of the carbonic and aqueous phases, and range from 0.83 to 0.94 g/cc. Furthermore, bulk chemical compositions of type II inclusions were calculated from data on the densities, volumes and relative fractions of the carbonic and aqueous phases. The calculated mole fractions of carbonic phase in type II inclusions (X_{CO2}+X_{CH4}) range from 0.05 to 0.78 (type IIa, 0.49 to 0.78; type IIb, 0.05 to 0.23).

Fluid immiscibility

As described above, hydrothermal fluids trapped in vein quartz as P+PS inclusions consist of two types: (1) a carbonic (CO_2- and CH_4-rich) fluid (type II); (2) an aqueous fluid with minor amounts of CO_2 (type Ia). Type II inclusions are quite variable in the carbonic content within individual samples. However, the homogenization temperatures of type IIa ($CO_2 < H_2O$) and type IIb ($CO_2 > H_2O$) inclusions have the similar range within frequency diagrams (Fig. 5). These observations indicate that fluid unmixing accompanying CO_2 effervescence was a major history of fluid evolution during the fluid entrapment.

It is noteworthy that gold grains and sulfide minerals occur mostly within fractures cutting quartz matrix. Therefore, the fluids responsible for gold deposition might have trapped as secondary or pseudosecondary inclusions in vein quartz. The secondary or psedosecondary inclusions occur characteristically as dominantly aqueous inclusions (type I). The carbonic inclusions (type II) are thought to have been trapped mostly prior to gold deposition, because they occur mostly as primary-like inclusions in quartz. We consider that the compositional change of hydrothermal fluids from largely carbonic toward aqueous fluids occurred due to extensive unmixing of fluids and was related to the deposition of gold and sulfides. The fluid inclusions with the Th-total data around 250°C are thought to record the unmixed fluids during the main gold deposition.

The relationships between Th-total data and salinity of P+PS inclusions are unclear, possibly suggesting the heterogeneity of hydrothermal fluids due to the fluid unmixing over the temperature range 250° to 370°C (Fig. 8). Some secondary aqueous inclusions with high salinity (>6 to about 12 wt. % NaCl equiv.) are thought to have been trapped successively from later unmixed fluids.

Experimental data on the system H_2O-CO_2(-CH_4)-NaCl may support the history of fluid unmixing. Fig. 9 shows the relations between the estimated compositions of type II fluid inclusions and the two-phase regions for the systems H_2O-CO_2(-CH_4)-NaCl at different salinity and pressure conditions. Not only the decreasing pressure but also the addition of CH_4 and/or NaCl raise the two-phase region of the H_2O-CO_2 system to higher temperatures (Takenouchi, Kennedy, 1965; Danneil *et al.*, 1967; Gehrig, 1980; Hendel, Hollister, 1981; Hollister *et al.*, 1981; Bowers, Helgeson, 1983). Our data plots mostly fall in the region between the H_2O-CO_2-6 wt. % NaCl (2 kbar) solvus and H_2O-CO_2-CH_4-6 wt. % NaCl (1 kbar) solvus but approach the H_2O-CO_2-6 wt. % NaCl (2 kbar) solvus, and show a compositional immiscibility

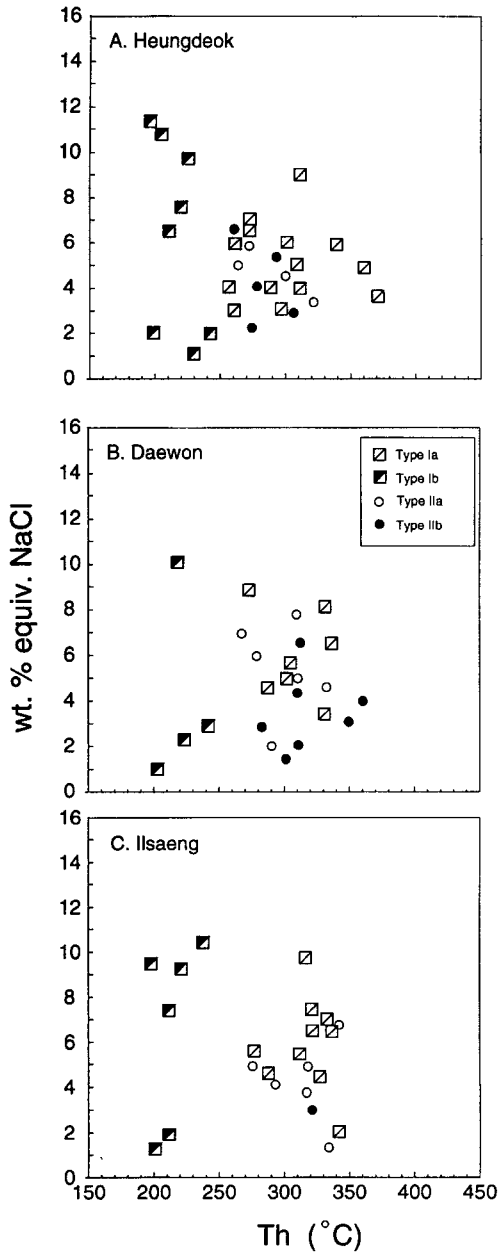

Fig. 8. Total homogenization temperature versus salinity relationships for fluid inclusions in vein quartz. Symbols of fluid inclusion type are the same as in Fig. 4.

gap at the range of $X_{CO2+CH4}$=0.25 to 0.5 (Fig. 9). Therefore, this approach gives an additional evidence of fluid unmixing. If considered the presence of CH_4 in type II inclusions, which raises the two-phase curve to higher temperatures, the approach of our data to the H_2O-CO_2-6 wt. % NaCl (2 kbar)

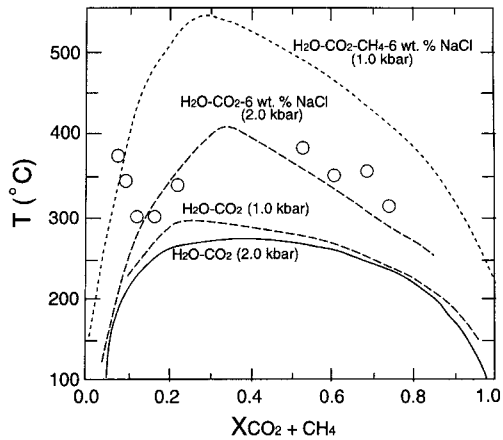

Fig. 9. Temperature versus bulk composition ($X_{CO2+CH4}$) diagram showing the solvus curves for the system H_2O-CO_2(-CH_4-NaCl) at different pressure and salinity conditions (after Danniel *et al.*, 1967; Gehrig, 1980; Bowers, Helgeson, 1983). Data plots shows the trapping conditions of type II inclusions in vein quartz.

solvus suggests the pressures around 2 kbars (or slightly higher).

For the unmixed fluid, the Th-total data of coexisting H_2O-rich and CO_2-rich inclusions generally correspond to the trapping temperatures of these fluids (Roedder, Bodnar, 1980). Assuming that the type II inclusion fluids simply belong to the H_2O + CO_2 + NaCl system, we can obtain the pressures of about 1.3 to 1.9 kbars for the fluid unmixing by the intersection between the calculated isochores (0.83~0.94 g/cc) for type II inclusions and the solvus curve for the system H_2O+10 mole % CO_2+4 wt. % NaCl (Bowers, Helgeson, 1983). The intersection points also indicate the temperatures of about 340° to 380°C, which fall in the range of Th-total data for type II inclusions. However, these pressures (1.3~1.9 kbars) should be considered as minimum estimates because the fluids actually contain minor amounts of CH_4. Therefore, we suggest that pressures during the deposition of quartz were at least 2 kbars.

STABLE ISOTOPES

We measured sulfur isotope compositions of sulfides, oxygen isotope compositions of quartz, and hydrogen isotope compositions of fluid inclusion waters. Standard techniques were used for extraction and analysis, as described by Grinenko

Table 2. Sulfur isotope data of sulfide minerals from Au deposits in the Youngdong area of the central Sobaegsan Massif.

Mine	Sample no.	Mineral	$\delta^{34}S$ (‰)	$\Delta^{34}S$ (‰)[1]	T (°C)[2]
Heungdeok	HD 1	sphalerite	0.5		
	HD 2	galena	-0.4		
	HD 3	pyrrhotite	1.2		
	HD 4-1	sphalerite	0.3	2.1	313±45
	HD 4-2	galena	-1.8		
	HD 6	pyrrhotite	0.7		
	HD 11	pyrrhotite	-1.4		
	HD 28-1	sphalerite	-1.0		
	HD 28-2	pyrrhotite	-0.9		
	HD 28-3	galena	0.9		
	HD 29	pyrrhotite	-1.4		
	HD 97-1	sphalerite	0.1	2.2	300±45
	HD 97-2	galena	-2.1		
Daewon	DW 1-1	pyrrhotite	1.2		
	DW 1-2	pyrrhotite	2.2		
	DW 2	pyrite	1.6		
	DW 3	galena	-1.5		
	DW 9	galena	1.0		
	DW 97-1	pyrrhotite	1.4		
Ilsaeng	IL 1	pyrrhotite	1.0		
	Il 10	pyrite	1.4		

[1] The observed sulfur isotopic fractionation between sphalerite and galena.
[2] Using sulfur isotope fraction equations in Ohmoto and Rye (1979).

Table 3. Oxygen and hydrogen isotope data of quartz and their inclusion fluids from Au deposits in the Youngdong area of the central Sobaegs\an Massif.

Mine	Sample no.	Mineral	$\delta^{34}O$ (‰)	T (°C)[1]	$\delta^{34}O_{water}$ (‰)[2]	δD (‰)
Heungdoek	HD 1-1	quartz	12.8	300	5.9	-7.7
	HD 1-2	quartz	11.8	300	4.9	-77
	HD 51	quartz	14.9	360	9.0	-6.8
	HD 7	quartz	14.1	370	9.3	-7.2
	HD 11	quartz	13.7	310	7.2	-7.4
	HD 28	quartz	12.6	290	5.4	-72
Daewon	DW 1	quartz	11.9	320	5.7	-75
	DW 4-1	quartz	13.2	310	6.7	-6.3
	Dw 4-2	quartz	11.9	300	5.0	-76
	Dw 9	quartz	12.6	330	6.7	-74
	Dw 97-1	quartz	12.5	340	6.9	-
Ilsang	Il 1	quartz	14.8	370	9.0	-79
	Il 2	quartz	11.0	300	4.7	-78

[1] Based on fluid inclusion and/or sulfur isotope temperatures and paragenetic constraints.
[2] Calculated water compositions based on quartz-water oxygen isotope fractionation equation in Matsuhisa *et al.* (1979)

(1962), Hall and Friedman (1963) and Rye (1966). Isotope data are reported in notations relative to the CDT standard for sulfur and the Vienna SMOW standard for oxygen and hydrogen. The standard error of each analysis is about ±0.1‰ for S and O, and ±0.2‰ for H (Tables 2 and 3).

Sulfur isotope

Analyses of sulfur isotopes were performed on

twenty-one hand-picked sulfide minerals from the Heungdeok, Daewon and Ilsaeng mines. They have the following $\delta^{34}S$ values (Table 2): pyrrhotite, -1.4 to 2.2‰; pyrite, 1.4 to 1.6‰; sphalerite, -1.0 to 0.5‰; galena, -2.1 to 1.0‰. Two sphalerite-galena pairs have the $\Delta^{34}S$ values of 2.1 and 2.2‰, yielding the coprecipitation temperatures of 313° ±45°C and 300°±45°C (Ohmoto, Rye, 1979).

Because the sulfur isotope fractionations between H_2S and pyrrhotite or sphalerite are very small over the temperature range 200~400°C (Ohmoto, Rye, 1979), the $\delta^{34}S$ values of pyrrhotite and sphalerite (-1.4 to 2.2‰) can be considered as an approximation of $\delta^{34}S$ values of H_2S. Furthermore, these $\delta^{34}S_{H2S}$ values can be considered as an approximation of $\delta^{34}S$ values of total sulfur in ore fluids ($\delta^{34}S_{\Sigma S}$), because the ore mineral assemblage pyrrhotite+pyrite along with the alteration mineral assemblage sericite+quartz indicates the dominance of H_2S among dissolved sulfur species (Ohmoto, Rye, 1979). The $\delta^{34}S_{\Sigma S}$ values around -2 to 2‰ also may indicate the igneous origin for the sulfur source.

Compared with previous data on ore sulfurs from metallic ore deposits in Korea (So, Shelton, 1987a, b; Shelton *et al.*, 1988; So *et al.*, 1988, 1989a,b), our present data are slightly lower. Previous studies for Korean gold-silver deposits show not only the scarcity of negative (isotopically light) sulfur isotope values but also the common range of $\delta^{34}S_{\Sigma S}$ values falling within 3 to 9‰. The difference in $\delta^{34}S_{\Sigma S}$ values may reflect the different reservoir characteristics (e.g., oxidation potential) of the ore-associated igneous melts.

Oxygen and hydrogen isotopes

Analyses of oxygen and hydrogen isotopes were performed on thirteen quartz samples and their extracted inclusion waters (Table 3). Careful optical observations were undertaken for the selection of samples for hydrogen isotope analysis in order to minimize the percentage of fracture-controlled secondary inclusions. The $\delta^{18}O$ values of quartz samples range narrowly from 11.0 to 14.9‰. Hydrothermal fluid's $\delta^{18}O$ estimates can be calculated from the fluid inclusion temperatures and the fractionation equation of Matsuhisa *et al.* (1979). The calculated $\delta^{18}O_{water}$ values are 4.7 to 9.3‰. The D values of inclusion waters in quartz are -63 to -79‰.

Fig. 10 shows the measured and calculated isotopic compositions of hydrothermal fluids for the formation of the Heungdeok, Daewon and Ilsaeng gold mines. Our data significantly overlap the general magmatic water box, and do not overlap with the metamorphic water box and the seawater or meteoric water values (Taylor, 1979). We conclude that the hydrothermal fluids responsible for gold deposits of the Heungdeok, Daewon and Ilsaeng mines were derived magmatically (possibly from hidden granitoids).

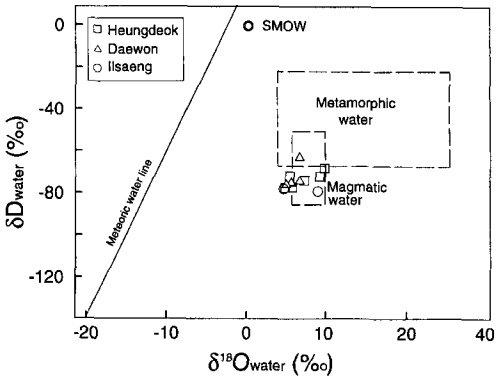

Fig. 10. A diagram showing hydrogen isotope (measured) and oxygen isotope (calculated from O isotope composition of quartz) compositions of hydrothermal fluids responsible for the formation of the Heungdeok, Daewon and Ilseang gold mines in the Youngdong area. The general magmatic and metamorphic water boxes are from Taylor (1979); the meteoric water line from Craig (1961).

SUMMARY

Gold-quartz veins of the Heungdeok, Daewon, and Ilsaeng mines in Youngdong area were examined for fluid inclusions and stable isotopes, in order to evaluate the successful application of a magmatic model for the genesis of mesothermal gold deposits in central Korea. Major conclusions of this study are summarized as follows:

1. Gold deposits of the studied mines occur as single stage of massive quartz veins (average gold grade=6 to 13 g/ton Au) which fill the fault shear zones in Precambrian metamorphic rocks of central Sobaegsan Massif. Hydrothermal wallrock alteration is weak and consists of low greenschist facies assemblage. The ore mineralogy is characterized by the dominance of pyrrhotite among iron sulfides and the gold-rich nature of electrums (74 to 83 atom. % Au).

2. Fluid inclusions in vein quartz comprise two main types: type I (aqueous liquid-rich) and type II (carbonic). Gold-quartz veins formed from mesothermal fluids with temperatures and salinities of 244° to 401°C and <9.5 wt. % NaCl equiv.,

respectively. The volume of carbonic phase in type II inclusions within a single quartz grain varies widely from about 10 to 90% at room temperature. Combined with the coexistence of type II inclusions with some type I inclusions, this observation indicates the occurrence of fluid's unmixing accompanying CO_2 effervescence. The overall compositional change of hydrothermal fluids from largely carbonic toward aqueous fluids occurred due to extensive unmixing of fluids and was related to the deposition of gold and sulfides.

3. Low melting temperatures (down to -63.3°C) and wide homogenization temperatures (8.4° to 29.7°C) of type II inclusions indicate the presence of appreciable CH_4 (2 to 20 mole %) in the carbonic phase. Mole fractions of the carbonic phase in type II inclusions ($X_{CO2}+X_{CH4}$) are calculated to fall in the wide range of 0.05 to 0.78. Plots of the homogenization temperature versus $X_{CO2+CH4}$ relationship for type II inclusions also indicate the occurrence of the fluid immiscibility with an immiscibility gap between $X_{CO2+CH4}$ values of 0.25 to 0.5 over the temperature range 250° to 370°C, and suggest the pressure conditions of >2 kbars for the mineralization. The homogenization temperature versus salinity relationships of fluid inclusions also indicate the fluid evolution comprising the early fluid's unmixing accompanying CO_2 effervescence and later cooling.

4. Stable isotope studies indicate that mesothermal gold mineralization of the Heungdeok, Daewon, and Ilsaeng mines occurred from the fluids with the $\delta^{34}S_{\Sigma S}$, $\delta^{18}O_{water}$ and δD_{water} values of -2.1 to 2.2‰, 4.7 to 9.3‰ and -63 to -79‰, respectively. These data indicate the magmatic origin of the mesothermal fluids. The occurrence, mineralogy, and fluid inclusion and stable isotope data of the studied three mines are quite comparable to those of the nearby Samhwanghak gold mine (So, Yun, 1997) and of mesothermal gold deposits in the eastern and northern edge parts of the Sino-Korean platform (Trumbull *et al.*, 1992; Miller *et al.*, 1998; Yao *et al.*, 1999), and may validate the applicability of a magmatic model for the genesis of these mesothermal gold deposits.

ACKNOWLEDGEMENTS

This study was financially supported by the Center for Mineral Resources Research (CMR). Constructive comments on the manuscript by Professors I.S. Lee (Seoul National Univ.) and H.K. Lee (Chungnam National Univ.) are greatly acknowledged.

REFERENCES

Angus, S., Armstrong, B., de Reuk, K.M., Altunin, V.V., Gadetskii, O.G., Chapala, G.A. and Rowlinson, J.S. (1973) International Thermodynamic Tables of the Fluid State: Carbon Dioxide. New York, Pergamon Press, 386 p.

Bodnar, R.J. (1993) Revised equation and table for determining the freezing point depression of H_2O-NaCl solutions. Geochim. Cosmochim. Acta, v. 57, p. 683-684.

Borisenko, A.S. (1977) Study of the salt composition of solutions in gas-liquid inclusions in minerals by the cryometric method. Soviet Geol. & Geophys., v. 18, p. 11-19.

Bowers, T.S. and Helgeson, H.C. (1983) Calculation of thermodynamic and geochemical consequences of nonideal mixing in the system H_2O-CO_2-NaCl on phase relations in geologic systems: Equation of state for H_2O-CO_2-NaCl fluids at high pressures and temperatures. Geochim. Cosmochim. Acta, v. 47, p. 1247-1275.

Bozzo, A.T., Chen, H.S., Kass, J.R. and Barduhn, A.J. (1975) The properties of hydrates of chlorine and carbon dioxide. Desalination, v. 16, p. 303-320.

Burrows, D.R., Wood, P.C. and Spooner, E.T.C. (1986) Carbon isotope evidence for a magmatic origin for Archean gold-quartz vein ore deposits. Nature, v. 321, p. 851-854.

Burruss, R.C. (1981) Analysis of phase equilibria in C-O-H-S fluid inclusions. Mineralog. Assoc. Canada Short Course Handb., v. 6, p. 39-74.

Choo, S.H. and Kim, S.J. (1985) A study of Rb-Sr age determinations on the Ryeongnam Massif (I): Pyeonghae, Buncheon and Kimcheon granite gneisses. Annual Report 85-24, Korea Inst. Energy and Resources, p. 7-39 (in Korean).

Craig, H. (1961) Isotopic variations in meteoric waters. Science, v. 133, p. 1702-1703.

Crawford, M.L. (1981) Phase equilibria in aqueous fluid inclusions. Mineralog. Assoc. Canada Short Course Handb., v. 6, p. 75-100.

Danneil, A., Tödheide, K. and Frank, E.W. (1967) Verdamptung gleichgewichte and kritiesche curven in den systemen attan/wasser und n-butan/wasser bei hohen drucken. Chemisch Ingenieurwesen Technik, p. 816-822.

Diamond, L.W. (1992) Stability of CO_2-clathrate hydrate+CO_2 liquid+CO_2 vapor+aqueous KCl-NaCl solutions: Experimental determination and application to salinity estimates of fluid inclusions. Geochim. Cosmochim. Acta, v. 56, p. 273-280.

Gehrig, M. (1980) Phasengleichgewichte und PVT-daten ternarer mischungen aus wasser, kohlendioxid und natrium chrolid bis 3 kbar und 550. Unpub. Ph.D. dissertation, Universitat Karlsruhe, Hochschul Verlag, Freiberg.

Grinenko, V.A. (1962) Preparation of sulfur dioxide for isotopic analysis. Zeitschr. Neorgan. Khimii, v. 7, p. 2478-2483.

Hall, W.E. and Friedman, I. (1963) Composition of fluid inclusions, Cave-in-Rock fluorite district, Illinois and Upper Mississippi Valley zinc-lead district. Econ. Geol., v. 58, p. 886-911.

Hedenquist, J.W. and Henley, R.W. (1985) The importance of CO_2 on freezing point measurements of fluid inclusions: evidence from active geothermal systems and implications for epithermal ore deposition. Econ. Geol., v. 80, p. 1379-1406.

Hendel, E.M. and Hollister, L.S. (1981) An empirical solvus for CO_2-H_2O-2.6 wt. % salt. Geochim. Cosmochim. Acta, v. 45, p. 225-228.

Heyen, G., Ramboz, C. and Dubessy, J. (1982) Simulation des equilibres anden phases daus le systeme CO_2-CH_4 en dessous de 50 et de 100bars: Application aux inclusions fluides. l'Academie des Sciences Computes Rendus [Paris], v. 294, series II, p. 203-206.

Hollister, L.S. (1981) Information intrinsically available from fluid inclusions. Mineralog. Assoc. Canada Short Course Handb., v. 6, p. 1-12.

Hollister, L.S. and Burruss, R.C. (1976) Phase equilibria in fluid inclusions from the Khtada Lake metamorphic complex. Geochim. Cosmochim. Acta, v. 40, p. 163-175.

Hollister, L.S., Crawford, M.L., Roedder, E., Burruss, R.C., Spooner, E.T.C. and Touret, J. (1981) Practical aspects of microthermometry. Mineralog. Assoc. Canada Short Course Handbook., v. 6, p. 278-301.

Kim, Y.I., Lee, K.H., Kim, D.M., Choi, G., Kim, J.W. and Cho, Y.S. (1982) Atlas of Gold deposits in Korea. KIER, 606p (in Korean).

Matsuhisa, Y., Goldsmith, J.R. and Clayton, R.N. (1979) Oxygen isotopic fractionation in the system quartz-albite-anorthite-water. Geochim. Cosmochim. Acta, v. 43, p. 1131-1140.

Miller, L.D., Goldfarb, R.J., Nie, F.J., Hart, C.J.R., Miller, M.L., Yang, Y.Q. and Liu, Y.Q. (1998) North China gold: a product of multiple orogens. Society of Economic Geologists Newsletter, v. 33, no. 1, p. 6-12.

Nesbitt, B.E. and Muehlenbachs, K. (1989) Geology, geochemistry, and genesis of mesothermal lode gold deposits of the Canadian Cordillera: evidence for ore formation from evolved meteoric water. Economic Geology Monograph, v. 6, p. 553-563.

Ohmoto, H. and Rye, R,O. (1979) Isotopes of sulfur and carbon, in Barnes, H.L., ed., Geochemistry of hydrothermal ore deposits. New York, Wiley Intersci., p. 509-567.

Roedder, E. (1984) Origin of fluid inclusions and changes that occur after trapping. Mineralog. Assoc. Canada Short Course Handb., v. 6, p. 101-137.

Roedder, E. and Bodnar, R.J. (1980) Geologic pressure determinations from fluid inclusion studies. Ann. Rev. Earth Planet. Sci., v. 8, p. 263-301.

Rye, R.O. (1966) The carbon, hydrogen, and oxygen isotopic compositions of hydrothermal fluids responsible for the lead-zinc deposits at Providencia, Zacatecas, Mexico. Econ. Geol., v. 61, p. 1339-1427.

Shelton, K.L., So, C.S. and Chang, J.S. (1988) Gold-rich mesothermal vein deposits of the Republic of Korea: Geochemical studies of the Jungwon gold area. Econ. Geol., v. 83, p. 1221-1237.

So, C.S. and Shelton, K.L. (1987a) Stable isotope and fluid inclusion studies of gold and silver bearing hydrothermal vein deposits, Cheonan-Cheongyang-Nonsan mining district, Republic of Korea: Cheonan area. Econ. Geol., v. 82, p. 987-1000.

So, C.S. and Shelton, K.L. (1987b) Fluid inclusion and stable isotope studies of gold-silver-bearing hydrothermal vein deposits, Yeoju mining district, Republic of Korea. Econ. Geol., v. 82, p. 1309-1318.

So, C.S. and Yun, S.T. (1997) Jurassic mesothermal gold mineralization of the Samhwanghak mine, Youngdong area, Republic of Korea: Constraints on hydrothermal fluid geochemistry. Econ. Geol., v. 92, p. 60-80.

So, C.S., Chi, S.J. and Choi, S.H. (1988) Geochemical studies on Au-Ag hydrothermal vein deposits, Republic of Korea: Jinan-Jeongeup mineralized area. Jour. Min. Pet. Econ. Geol. (Japan), v. 83, p. 449-471.

So, C.S., Choi, S.H., Lee, K.Y. and Shelton, K.L. (1989a) Geochemical studies of hydrothermal gold deposits, Republic of Korea: Yangpyeong-Weonju area. Jour. Korean Inst. Mining Geol., v. 22, p. 1-16.

So, C.S., Yun, S.T. and Chi, S.J. (1989b) Geochemical studies of hydrothermal gold-silver deposits, Republic of Korea: Yangdong mining district. Jour. Geol. Soc. Korea, v. 25, p. 16-29.

So, C.S., Yun, S.T. and Shelton, K.L. (1995) Mesothermal gold vein mineralization of the Samdong mine, Republic of Korea: A geochemical and fluid inclusion study. Mineral. Deposita, v. 30, p. 384-386.

Spooner, E.T.C. (1991) The magmatic model for the origin of Archean Au-quartz vein ore system: an assessment of the evidence, in Ladeira, E.A., Ed., Brazil Gold '91. Rotterdam, Balkema, p. 313-318.

Takenouchi, S. and Kennedy, G.C. (1965) The solubility of carbon dioxide in NaCl solutions at high temperatures and pressures. Am. Jour. Sci., v. 263, p. 445-454.

Taylor, H.P.Jr. (1979) Oxygen and hydrogen isotope relationships in hydrothermal mineral deposits, in Barnes, H.L., ed., Geochemistry of hydrothermal ore deposits. New York, Wiley Intersci., p. 236-277.

Trumbull, R.B., Morteani, G., Li, Z.L. and Bai, H.S. (1992) Gold metallogeny in the Sino-Korean platform. Springer-Verlag, Berlin, 202p.

Yao, Y., Morteani, G. and Trumbull, R.B. (1999) Fluid inclusion microthermometry and the P-T evolution of gold-bearing hydrothermal fluids in the Niuxinshan gold deposit, eastern Hebei province, NE China. Mineralium Deposita, v. 34, p. 348-365.

Yun, S.T. (1991) Gold-silver mineralizations in the Mooju-Youngdong mine district, Korea: a comparative geochemical study based on mineralogical, fluid inclusion, and stable isotope systematics. Ph.D thesis, Korea Univ., 372p.

Zhang, H.T., So, C.S. and Yun, S.T. (1999) Regional geologic setting and metallogenesis of central Inner Mongolia, China: guides for exploration of mesothermal gold deposits. Ore Geology Reviews, v. 14, p. 129-146.

1999년 6월 12일 원고접수, 1999년 9월 2일 게재승인.

소백산 육괴 중부 지역의 변성암에서 산출되는 중온형 금광상에 대한 유체 포유물 및 안정동위원소 연구: 영동 지역

소칠섭* · 윤성택* · 권순학*

요 약 : 소백산 육괴 중부 지역의 선캠브리아기 변성암류에는 특징적으로 중열수형 금광상이 다수 배태된다. 영동 지역의 흥덕 · 대원 · 일생 금 광산도 이에 속하며, 단층 열극을 충진한 괴상의 석영맥 (폭 0.3~3 m)으로 산출된다. 광석 광물은 매우 단순하여 주로 자류철석, 섬아연석, 방연석으로 산출되며, 황철석, 황동석, 엘렉트럼, 사면동석, 자연창연이 일부 수반된다. 유체포유물 연구 결과, 광화작용은 비교적 높은 온도 (240~400°C)에서 낮은 염농도 (<12 wt. % NaCl equiv.)를 갖는 H_2O-CO_2(-CH_4)-NaCl계 유체로부터 진행되었다. 석영 내의 유체포유물은 단순한 액상 포유물(Type I)과 메탄을 함유하는 CO_2-rich 포유물(Type II)로 구분된다. Type II 포유물의 carbonic phase (주로 CO_2)의 함량은 동일 시료 내에서도 매우 다양하게 변화하며, carbonic phase 내의 메탄 함량은 대략 2~20 mole %이다. 유체포유물의 균일화온도와 염농도의 관계를 보면, 광화작용의 초기에는 CO_2 비등을 수반한 유체 불혼화가 일어났으나, 후기에는 냉각작용이 지배적이었음을 알 수 있다. 광화작용시의 추정 압력은 최소 2 kbar의 고압을 나타낸다. 측정 또는 추정된 광화 유체의 유황 및 산소-수소 동위원소 조성 ($\delta^{34}S_{\Sigma S}$= -2.1 to 2.2‰, $\delta^{18}O_{water}$= 4.7 to 9.3‰, δD_{water}= -63 to -79‰)은 광화유체가 마그마로부터 기원하였음을 지시한다. 본 연구 결과는 영동지역에 부존하는 중온형 금광상의 성인에 대하여 마그마 기원 모델을 성공적으로 적용할 수 있음을 확인해준다.